LASER APPLICATIONS AND OTHER TOPICS IN QUANTUM ELECTRONICS

PACS numbers: 42.62.Fi; 42.25.Gy; 42.25.Ja
DOI: 10.1070/QE2009v039n06ABEH013773

Selective reflection of obliquely incident polarised light

Ya.A. Fofanov

***Abstract*. A series of reflection resonances formed by the hyperfine components of the D_2-lines in the spectrum of the natural mixture of rubidium isotopes is studied. Passages from resonantly frustrated total internal reflection to resonance Brewster reflection caused by the frequency tuning of the incident light are demonstrated experimentally. The contrast of the strongest refection resonances exceeds 500 % at the moderate heating of reflecting cells. The intensity of the reflected light changes in this case by more than 20 times. A theory is developed which is based on a two-level model for resonance atoms and Fresnel formulas for reflection coefficients. Numerical calculations based on the proposed theory confirm main experimental results.**

Keywords: *selective reflection, polarised light, laser, laser radiation noise*.

1. Introduction

Selective resonance reflection from a dielectric-resonance gas interface has been known from the beginning of the last century [1]. Later, sub-Doppler resonances in selective reflection at the angles of incidence close to zero were observed and theoretically explained [2 – 6]. The authors of papers [7 – 10] investigated the inclined geometry, when the angles of incidence were equal to the nonresonance value of the Brewster angle and also lied in the region of the critical total internal reflection (TIR) angle [7 – 10].

Interest in the selective reflection of light is related to the possibilities of its application in the spectroscopy of optically dense media [2 – 15]. This phenomenon is used for studying the impact line broadening [4, 16], for the development of selective elements of lasers [17 – 20], and for investigation of the interaction of excited atoms with solid surfaces, including the van der Waals interaction [21 – 23].

The aim of this paper is to study in detail the features of selective reflection of polarised light for a series of closely spaced lines under conditions close to the resonance TIR and resonance Brewster reflection (BR). The obtained results can be used in the spectroscopy of dense gases and in optical informatics and quantum optics to control the intensity of reflected light and reduce its fluctuations (including quantum fluctuations).

Ya.A. Fofanov Institute of Analytic Instrumentation, Russian Academy of Sciences, Rizhskii pr. 26, 190103 St. Petersburg, Russia; e-mail: Yakinvest@yandex.ru

Received 30 November 2007; revision received 11 February 2009
Kvantovaya Elektronika **39** (6) 585 – 590 (2009)
Translated by M.N. Sapozhnikov

2. Experimental method and results

The scheme of the experimental setup is shown in Fig. 1. As a radiation source a single-frequency 780-nm semiconductor laser was used, which was tuned to the hyperfine components of the D_2-line of rubidium isotopes [24]. The laser was tuned by varying the injection current. Laser radiation was directed on cells operating in absorption or reflection regimes. Absorption cells had a length of 50 mm and were kept at room temperature.

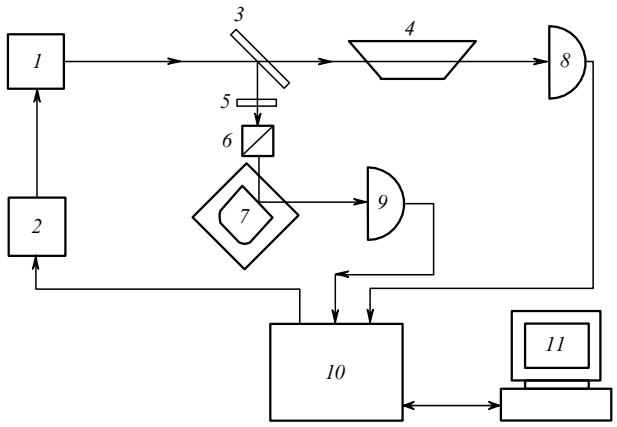

Figure 1. Scheme of the experimental setup: (*1*) laser; (*2*) laser power supply; (*3*) beamsplitter; (*4*) absorption cell; (*5*) $\lambda/4$ plate; (*6*) polariser; (*7*) reflection cell; (*8, 9*) photodiodes; (*10, 11*) detection and experiment control unit.

Laser radiation was incident on the entrance window of a reflection cell filled with saturated rubidium vapour. The reflection of light from the transparent dielectric-resonance gas interface was provided at an angle of incidence close to the Brewster angle and critical TIR angle. The concentration of resonance atoms in reflection cells was controlled by their heating up to 200 °C. We used the natural mixture of ^{85}Rb and ^{87}Rb isotopes. The orientation of the polarisation plane of linearly polarised laser radiation was varied with the help of a polariser. The laser radiation power density in the absorption cell and at the interface under study was considerably lower than the saturation power density.

Reflection cells used in experiments were equipped with a system for radiation input/output, which provided operating conditions close to TIR. However, unfortunately the measurement accuracy of the angles of incidence restricted by the properties of this system was only $\pm 0.5^\circ$ (see section 3). Other experimental factors such as the laser beam divergence, the quality of reflecting surfaces, adjustment errors, etc. introduced considerably smaller contributions. For these reasons, the angular position of reflection cells was set by the value of the nonresonance reflection coefficient.

Figures 2a and c show three typical dependences of the reflection coefficient on the laser frequency (reflection spectra). These dependences correspond to three different angles of incidence and two orientations of the polarisation plane – parallel to the plane of incidence (parallel orientation) and orthogonally to the plane of incidence (orthogonal orientation). Figures 2b, d show the relative intensity of light transmitted through the absorption cell (absorption spectra). The hyperfine components of D_2-lines of ^{85}Rb and ^{87}Rb isotopes correspond to peaks a, A, B, and b in absorption spectra, which were used to calibrate frequency axes.

The shapes of reflection curves (*1–3*) noticeably differ from each other. Reflection spectra (*1*) in Figs 2a and c correspond to the angle of incidence 64° at which TIR conditions are fulfilled outside resonance lines (or in the absence of gas) (the nonresonance critical TIR angle is 34.6°). One can see that these curves virtually coincide with the absorption curves, exhibiting dips a′, A′, B′, and b′ at resonance lines, which are similar to dips a, A, B, and b in absorption spectra. This suggests that the dips in curves (*1*) are formed by the violation of TIR due to the absorption of laser radiation by resonance gas. Radiation is absorbed by atoms interacting with a surface light wave existing under TIR conditions [25].

Reflection spectra (*2*) in Figs 2a and c correspond to the angle of incidence 34° at which resonance TIR conditions are not fulfilled outside resonance lines and the nonresonance reflection coefficient is 0.40 and 0.75 for parallel orientation and orthogonal orientations, respectively. Curves (*2*) strongly differ from curves (*1*) and (*4*). One can see that the reflection coefficient at the bottom of dips a′, A′, B′, and b′ considerably decreased and reflection peaks a″, A″, B″, and b″ appeared. The formation of reflection peaks is especially well observed by comparing peaks A″, B″, and b″. The tops of peaks b″ are still flat because conditions close to frustrated TIR (FTIR) are fulfilled at their frequencies. The reflection coefficient at the tops of peaks A″ and B″ is somewhat smaller, and these tops are sharper. Peaks a″ in all curves are weaker, which can be explained by the influence of adjacent peak A″.

By comparing reflection spectra (*2*) (Figs 2a and c), we see that the reflection coefficient at the bottom of dips a′, A′, B′, and b′, corresponding to the parallel orientation (Fig. 2a), is several times smaller than that in the reflection spectrum for orthogonal orientation (Fig. 2c). This can be explained by the fact that reflection conditions at the bottom of dips in Fig. 2a approach to BR, more exactly to pseudo-BR (PBR) because resonance gas has absorption. At the same time, it is known that BR and PBR do not exist in the case of orthogonal polarisation.

The approach to PBR in curve (*2*) (Fig. 2a) occurs to the resonance change in the refraction index of an atomic ensemble and the corresponding modification of the Brewster angle. In this case, the intensity of reflected light considerably changes. The most significant change (by more than 5 times) is observed at the left wing of peak A″.

Spectra (*3*) in Figs 2a and c demonstrate pronounced resonance reflection in the inclined geometry. These spectra correspond to the angle of incidence 33° at which the reflection coefficient outside resonance lines is 0.10 and 0.50 for the parallel and orthogonal orientations, respectively. A comparison of peaks (*2*) and (*3*) in Figs 2a and c shows that the intensities of peaks A″ and B″ for both orientations decrease with decreasing the angle of incidence, which is mainly explained by the deviation from conditions close to TIR. Nevertheless, the resonance reflection coefficient at the top of peak B″ of spectrum (*3*) in Fig. 2a exceeds 60 %, while the contrast of this resonance (the ratio of the peak intensity to the pedestal intensity) is no less than five. At the same time, the reflection conditions at dips a′, A′, B′ and b′ in spectrum (*3*) in Fig. 2a are much closer to TIR than in spectrum (*2*). As a result, the reflection coefficient drastically changes on passing from the tops of peaks to dips between them. This change for peaks A″ and B″ in spectrum (*3*) in Fig. 2a exceeds 20 and 10, respectively.

By estimating the degree of approaching to TIR in spectra in Fig. 2a, note that the angle of incidence for spectra (*2*) and (*3*) is greater by 4.4° and 3.4°, respectively, than the nonresonance Brewster angle (29.6°), and therefore reflection conditions outside resonances in spectra (*2*) and (*3*) are far from BR. This is also confirmed by nonresonance reflection coefficients for these spectra, which are equal to 0.4 and 0.1, respectively, whereas refection coefficients at the bottom of dips A′ in spectra (*2*) and (*3*) are 2.2 and 4.1 times smaller. At the same time, reflection coefficients at the bottom of dips A′ in spectra (*2*) and (*3*) in Fig. 2c are smaller than the corresponding resonance coefficients only by 1.3 and 1.4 times. Thus, as the incident light frequency is tuned, a passage to reflection conditions approaching TIR is observed in spectra (*2*) and (*3*) in Fig. 2a.

3. Theoretical model and calculation results

The theoretical consideration is based on the model of a two-level atom interacting with a plane light wave. It is assumed that the atom has only the ground state and one excited state no transitions occurs to other levels and the resonance transition is not saturated by a laser field. Based on expressions for the density matrix, corrections to the wave vector k of a resonance light wave, which are determined by an ensemble of atoms, are found [26]:

$$\Delta k = \Delta k' + \mathrm{i}\Delta k'', \tag{1}$$

$$\Delta k' = -\Delta\mu\Delta k'', \tag{2}$$

$$\Delta k'' = \frac{k_0'' n_0 f}{\Gamma_{21}(1+\Delta\mu^2)}, \tag{3}$$

where n_0 is the concentration of atoms; f is the oscillator strength; Γ_{21} is the homogeneous half-width of the atomic line; $\Delta\mu = (\nu - \nu_a)/\Gamma_{21}$ is the dimensionless detuning of the field frequency ν from the atomic frequency ν_a; and k_0'' is a numerical coefficient determined by fundamental constants and the chosen system of units.

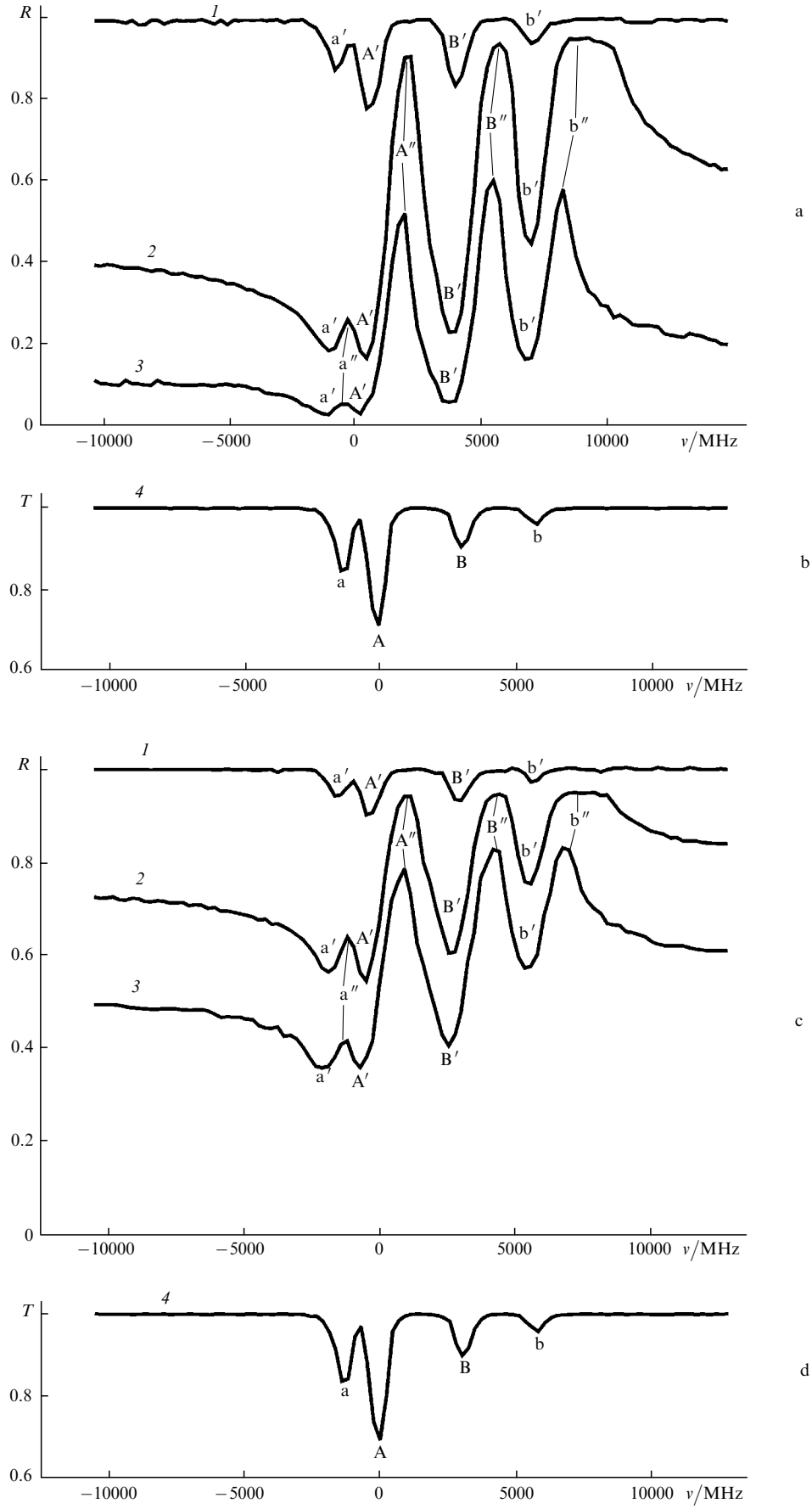

Figure 2. Experimental reflection (a, c) and absorption (b, d) spectra for light with polarisation planes parallel (a) and orthogonal (c) to the plane of incidence for angles of incidence 64° (*1*), 34° (*2*), and 33° (*3*), respectively, and the atomic concentration $n_0 = 2 \times 10^{15}$ (a, c) and 3.3×10^9 cm^{-3} (b, d). The zero detuning frequency corresponds to the positions of dip A in curve (*4*).

The real experimental situation, in which selective reflection was determined by four resonance lines, was described by calculating the total correction to the wave vector

$$\Delta k = \sum_{k=1}^{4} g_i \Delta k_i, \tag{4}$$

where g_i is a factor taking into account the concentration ratio of rubidium isotopes and multiplicity of levels. It is assumed that the population of Zeeman and hyperfine sublevels is equilibrium.

Then, the value of $\langle \Delta k \rangle_{\mathrm{D}}$ was determined by averaging over the Doppler distribution of atomic frequencies and the refractive index of the atomic gas was found:

$$n_2 = 1 + \langle \Delta k \rangle_{\mathrm{D}} / k. \tag{5}$$

The intensity reflection coefficients for parallel and orthogonal orientations of the polarisation plane were determined by Fresnel formulas

$$R_{\parallel} = \left| \frac{(n_2/n_1)^2 \cos\theta - [(n_2/n_1)^2 - \sin^2\theta]^{1/2}}{(n_2/n_1)^2 \cos\theta + [(n_2/n_1)^2 - \sin^2\theta]^{1/2}} \right|^2, \tag{6}$$

$$R_{\perp} = \left| \frac{\cos\theta - [(n_2/n_1)^2 - \sin^2\theta]^{1/2}}{\cos\theta + [(n_2/n_1)^2 - \sin^2\theta]^{1/2}} \right|^2, \tag{7}$$

where n_1 is the refractive index of the reflection cell window and θ is the angle of incidence.

The results of calculations for parallel and orthogonal orientations are presented in Fig. 3. By comparing the experimental data and theoretical calculations, it is necessary to take into account that the intensity of resonances in the region between the critical TIR angle and Brewster angle strongly depend on the angle of incidence. Unfortunately, cells used in our experiments prevented the measurement of the angles of incidence with the required accuracy (0.1°–0.2° and better, see section 1).

To compare calculated and experimental results, the values of θ in (6) were selected for each of the curves (*1–3*) in Fig. 3a so that the theoretical values of the absorption coefficient at the bottom of dips B′ in curve (*1*) and the reflection coefficient at maxima of peaks B″ in curves (*2*) and (*3*) coincided with the corresponding experimental values in curves (*1–3*) in Fig. 2a; the same value of θ were then substituted into (7) to construct each of the curves in Fig. 3b. This allows us to compare theoretical and experimental data obtained for both orientations of the polarisation plane.

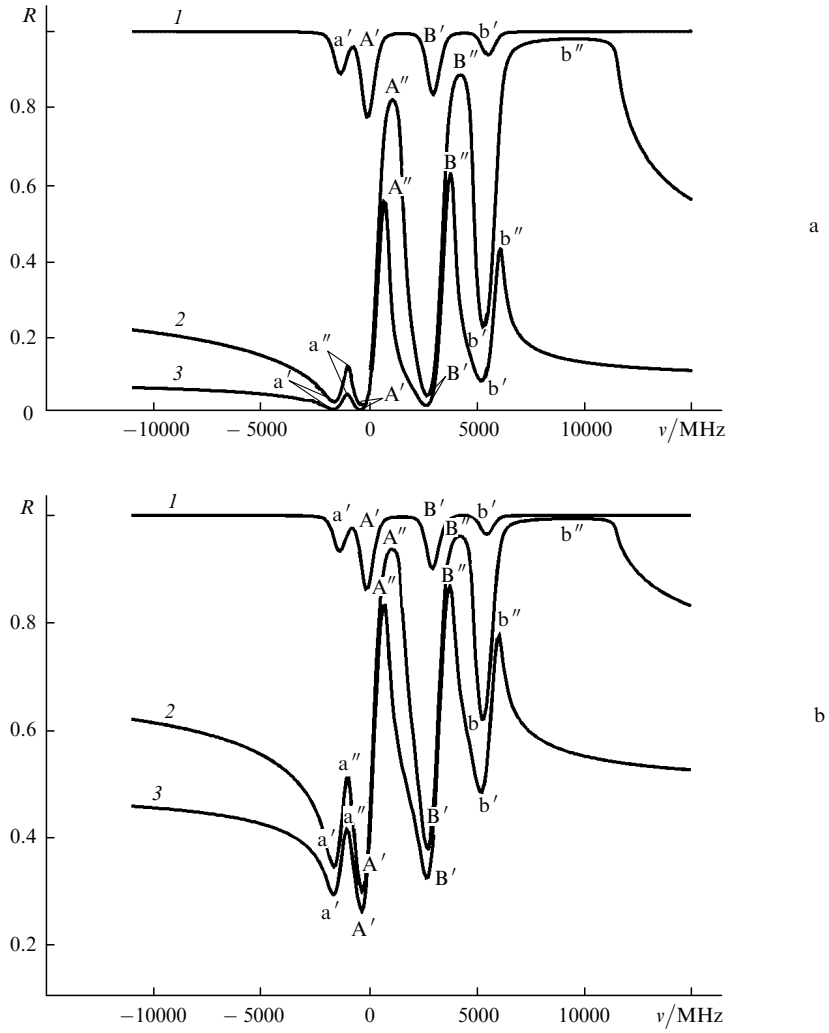

Figure 3. Calculated reflection spectra for light with parallel (a) and orthogonal (b) polarisation planes for $\theta = 65°$ (*1*), 34.3° (*2*), and 33.3° (*3*).

One can see that theoretical curves are in well agreement with experimental curves, demonstrating the high contrast and the greater intensity of reflection resonances. The curves describing the reflection coefficient for light with the polarisation plane parallel to the plane of incidence lie below the curves with the orthogonal polarisation plane and the intensity of reflected light at the bottom of dips for the former curves is considerably smaller. This confirms the fact that for light with the parallel orientation of the polarisation plane, the resonance passage from nearly TIR conditions to PBR conditions exists.

Note that there exist differences between experimental and theoretical results. Thus, the width of the flat top of peak b″ on experimental curves (*2*) (Fig. 2) is noticeable smaller than that on calculated curves (*2*) (Fig. 3). In addition, the maximum value of the reflection coefficient at peaks A″ is greater than at peaks b″ on calculated curves (*3*), while in experiments the situation is inverse. These and other similar discrepancies can be explained first of all by the simplicity of the theoretical model used, which is based on the description of the optical properties of resonance gas with the help of the refractive index. A more detailed theoretical analysis requires the use of theoretical approaches developed, for example, in [3, 5, 6, 12, 14, 15, 23]. This will probably make it possible to obtain from experimental reflection spectra new information on the interaction of atoms with resonance radiation near surfaces [23].

Note also that the curves in Fig. 2, especially curves (*4*) exhibit angularities. They are caused by the use of an external diffraction-grating cavity laser, which is intended for other studies [24]. The external cavity of this laser was misaligned to provide continuous tuning in the required range. The 'angularity' of the experimental spectra is caused by the insufficient misalignment of the diffraction grating resulting in a partial locking of the laser frequency by the external cavity (the superweak coupling regime [24]). In addition, errors in the mapping of calculated data also made some contribution [see, for example, 'angularities' of peaks A″ and b″in curves (*2–3*) in Fig. 3]. However, this does not affect the basic results obtained in the paper.

4. Conclusions

A series of reflection resonances formed by the hyperfine components of the D_2-lines of the natural mixture of ^{85}Rb and ^{87}Rb isotopes has been investigated. It is expedient to compare the obtained results with the results of other authors.

In [7], a cell with mercury vapour was illuminated by the 253.5-nm radiation incident at the Brewster angle. In this case, the maximum selective reflection coefficient was 14 %. Strong reflection resonances in rubidium and cesium vapours at the angles of incidence close or equal to the Brewster angle were first observed in [9]. In the case of parallel orientation of the polarisation plane in the presence of resonance atoms, the passage from BR to FTIR was observed. The reflection coefficient increased up to 95 %, which exceeded the nonresonance reflection coefficient by an order of magnitude. Such a strong reflection was caused by high concentrations of atoms, which were achieved by heating a cell up to 350°. Note that a strong heating can present problems with the design and service life of reflection cells. Increasing air flows in the optical path and thermal deformations of cell mounts increase fluctuations of parameters of a reflected beam, which poses additional difficulties in studies of the reflected light statistics.

In this paper, comparative investigations of resonance reflection from rubidium vapour were performed for light with parallel and orthogonal orientations of the polarisation plane. By varying the angle of incidence, the initial (nonresonance) reflection conditions were controlled from TIR to conditions close to BR. At the angles of incidence exceeding the critical TIR angle, the violation of TIR was observed within a series of resonances for both polarisations, which was caused by the resonance absorption of coherent radiation by atoms interacting with a surface light wave. Such effects were observed earlier at concentrations of sodium atoms $\sim 10^{16}$ cm^{-3} [25]. The sensitivity of the experimental setup described in the present paper allows the detection of resonance FTIR at atomic densities 10^{14} cm^{-3} and lower.

If the angle of incidence was chosen so that nonresonance reflection conditions were intermediate between TIR and BR and the polarisation plane of incident radiation was parallel to the plane of incidence, the tuning of laser radiation was accompanied by the passage from reflection conditions typical for resonance FTIR to conditions close to resonance PBR. In this case, the intensity of the strongest reflection resonances increases by more than five times.

In [8], selective reflection from sodium vapour was investigated at low concentrations, when the homogeneous linewidth is smaller than the Doppler width. For the angle of incidence of 83°, the maximum reflection coefficient was ~ 77 % and the contrast was 1.15. In our conditions, the contrast of the strongest reflection resonances exceeded five. This is approximately six times greater than in the case of sub-Doppler resonances in the orthogonal geometry at the same concentrations of resonance atoms [4]. In experiments described here, more than 60 % of the incident light was reflected in strong maxima. To obtain comparable reflection in the orthogonal geometry, atomic concentrations should be a few orders of magnitude higher [11], which considerably complicates the design of reflection cells. At atomic concentrations comparable with these used in the present paper, the maximum reflection coefficient in the orthogonal configuration was 8 % [4]. At the same time, the contrast of resonances that we observed was four times smaller than that in [9], which is explained by a lower concentration of resonance atoms in our study. In [26], the shift and broadening of the hyperfine structure of the D_2-line in dense rubidium vapour were studied under FTIR conditions.

Aside from a high contrast, many applications (for example, the laser line frequency stabilisation) require narrow resonances and the absence of the frequency shift with respect to the unperturbed transition frequency. As applied to selective reflection, sub-Doppler resonances observed upon orthogonal incidence have these properties to some extent [4]. Sub-Doppler resonances are also observed in extremely thin cells [23].

Our experiments did not reveal sub-Doppler resonances in the inclined geometry. Sub-Doppler reflection resonances in sodium vapour under FTIR conditions observed in [13] were caused by the absorption and dispersion saturation in a counterpropagating surface wave. The contrast of resonances was ~ 0.01 %. Reflection resonances described in the present paper are a few orders of magnitude stronger and

are rather broad. This can be useful for solving other problems related, for example, to the transformation of light statistics because the negative influence of frequency fluctuations of probe laser radiation is noticeably reduced for broad reflection resonances, while the band of transmitted frequencies can be noticeably broadened [27].

The theory has been developed which is based on the Haken model for resonance atoms and Fresnel formulas for the reflection coefficient. The reflection coefficients are obtained for a series of closely spaced reflection resonances for the cases of parallel and orthogonal orientations of the polarisation plane of incident laser radiation. The calculated curves are in good agreement with experiments and correctly describe the basic features of experimental curves.

The selective reflection of polarised light can be used to control the intensity and fluctuations of reflected light, including the control of its quantum composition. The latter assumption is based on the nonlinear properties of reflection resonances determining the dependence of the selective reflection coefficient on the incident light intensity [27]. These effects were explained theoretically in [28]. Of interest are further studies of the interaction of light with resonance atoms in the case of Brewster reflection and in a surface wave, as well as the observation of bistability and formation of transverse structures in the system under study [29].

Acknowledgements. This work was partially supported by the Russian Foundation for Basic Research (Grant No. 06-02-17219-a).

References

1. Wood R.W. *Philos. Mag.*, **18**, 187 (1909).
2. Cojan J.L. *Ann. Phys. (Paris)*, **9**, 385 (1954).
3. Schurmans M.F.H. *J. Physique*, **37**, 469 (1976).
4. Sautenkov V.A., Velichasnsky V.L., Zibrov A.S., Luk'yanov V.I., Nikitin V.V., Tyurikov D.A. *Kvantovaya Elektron.*, **8**, 1867 (1981) [*Sov. J. Quantum Electron.*, **11**, 1131 (1981)].
5. Nienhuis G., Schuller F., Ducloy M. *Phys. Rev. A*, **38**, 5197 (1988).
6. Vartanyan T.A. *Opt. Spektrosk.*, **68**, 625 (1990).
7. Senitzky B. *Appl. Phys. Lett.*, **24**, 68 (1974).
8. Burgmans A.L.J., Woerdman J.P. *J. Physique*, **37**, 677 (1976).
9. Akul'shin A.M., Velichansky V.L., Zherdev A.I., Zibrov A.S., Malakhova V.U., Nikitin V.V., Sautenkov V.A., Kharisov G.G. *Kvantovaya Elektron.*, **16**, 631 (1989) [*Sov. J. Quantum Electron.*, **19**, 416 (1989)].
10. Andreev A.V. *Pis'ma Zh. Tekh. Fiz.*, **12**, 1025 (1986).
11. Lauriston A.C., Welsh H.L. *Canad. J. Phys.*, **39**, 217 (1951).
12. Guo J., Cooper J., Gallagher A., Lewenstein M. *Opt. Commun.*, **110**, 197 (1994).
13. Simoneau P., Le Boiteaux S., De Arauio Cid B., Bloch D., Lios Leite I.R., Ducloy M. *Opt. Commun.*, **59**, 103 (1986).
14. Schuller F., Gorceix O., Ducloy M. *Phys. Rev. A*, **47**, 519 (1993).
15. Vartanyan T.A., Weis A. *Phys. Rev. A*, **63**, 1 (2001).
16. Akul'shin A.M., Velichansky V.L., Zibrov A.S., Nikitin V.V., Sautenkov V.A., Yurkin E.K., Senkov N.V. *Pis'ma Zh. Eksp. Teor. Fiz.*, **36**, 247 (1982).
17. Letokhov V.S. *Kr. Soobshch. Fiz. FIAN*, (11), 14 (1970).
18. Velichansky V.L., Zibrov A.S., Nikitin V.V., Sautenkov V.A., Malyshev V.K., Kharisov G.G. *Kvantovaya Elektron.*, **5**, 1465 (1978) [*Sov. J. Quantum Electron.*, **8**, 836 (1978)].
19. Akul'shin A.M., Velichansky V.L., Zverkov M.V., et al. *Kr. Soobshch. Fiz. FIAN*, (1), 47 (1986).
20. Ito T., Hashi T., Yabuzaki T. *Opt. Commun.*, **82**, 473 (1991).
21. Van Kampen H., Sautenkov V.A., Eliel E.R., Woerdman J.P. *Phys. Rev. A*, **58**, 4473 (1998).
22. Failache H., Saltiel S., Fichet M., Bloch D., Ducloy M. *Eur. Phys. J. D*, **23**, 237 (2003).
23. Bloch D., Ducloy M. *At. Mol. Opt. Phys.*, **50**, 1 (2005).
24. Fofanov Ya.A., Sokolov I.V. *J. Opt. Technol.*, **70**, 38 (2003).
25. Boissel P., Kerherve F. *Opt. Commun.*, **37**, 397 (1981).
26. Kondo R., Tojo S., Fujimoto T., Hasuo M. *Phys. Rev. A*, **73**, 062504 (2006).
27. Fofanov Ya.A. *Opt. Spektrosk.*, **99**, 457 (2005).
28. Belinskii A.V. *Kvantovaya Elektron.*, **18**, 84 (1991) [*Sov. J. Quantum Electron.*, **21**, 75 (1991)].
29. Rozanov N.N. *Opticheskaya bistabil'nost' i gisterezis v raspredelennykh nelineinykh sistemakh* (Optical Bistability and Hysteresis in Distributed Nonlinear Systems) (Moscow: Nauka, 1997).